The Study of PWM Methods in Permanent Magnet Brushless DC Motor Speed Control System

Qiang Li, Hai Huang, Binchuan Yin
Wuhan Marine Electric Propulsion Research Institute, wuhan, 430064, China

***Abstract*-The Permanent Magnet Brushless DC Motor Speed Control System（PMBDCSCS）is simple control, high power density and high performance, and used in many domains. The voltage inverter used widely in the PMBDCSCS operates commonly in the six PWM methods: H_PWM_L_PWM， ON_PWM，H_PWM_L_ON，H_ON_L_PWM，PWM_ON and PWM_ON_PWM. In this paper, the six PWM methods are introduced in theory and are compared in detail at the system level, the analysis is proved true by the simulation result.**

I. THEORY OF THE SIX PWM METHODS

The Permanent Magnet Brushless DC Motor Speed Control System(PMBDCSCS) which simplified diagram is shown in Fig.1 operates in 120^0 conduction mode, the controller according to rotor position signal sent from the rotor position sensor controls the turn-on and turn-off of power electronic devices. At any instant the duty cycle of power electronic devices in the PWM is changed to adjust the permanent magnet motor rotate speed. The logic trigger signal of each power electronic device in the different PWM method is showed in Fig.2 to Fig.7.

II. COMPARISON OF THE SIX PWM METHODS

A. Comparison of efficiency and reliability in the six PWM methods

Unlike the other five PWM methods, H_PWM_L_PWM is that the both devices in conduction are chopped at switching frequency, it has almost twice switching loss than the other five PWM methods. The inverter output voltage varies between U_d and $-U_d$ in H_PWM_L_PWM，therefore H_PWM_L_PWM is the bipolar control. However the inverter output voltage varies between U_d and zero in the other five PWM methods, therefore the other five PWM methods are the unipolar control. The switching frequency current pulsation in H_PWM_L_PWM is almost twice than in the other five PWM methods, the permanent motor in H_PWM_L_PWM has more harmonic loss. So H_PWM_L_PWM is the lowest in efficiency.

ACKNOWLEDGMENT

With the help of both teachers, I have finished this paper. Hereon Qiang Li sincerely thanks professor Binchuan Yin and senior engineer Hai Huang.

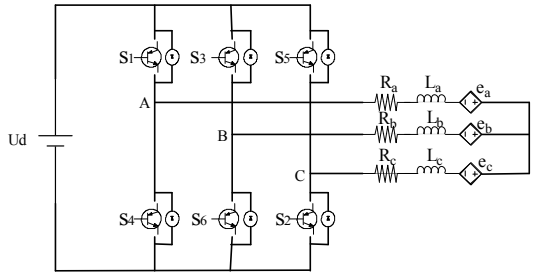

Fig.1. simplified diagram of PMBDCSCS

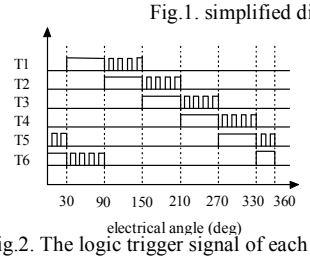

Fig.2. The logic trigger signal of each device in ON_PWM

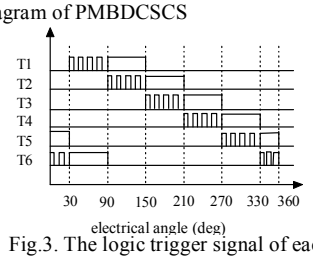

Fig.3. The logic trigger signal of each device in PWM_ ON

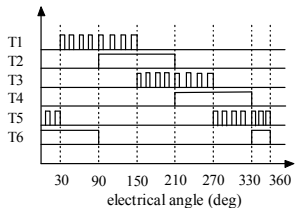

Fig.4. The logic trigger signal of each device in H_PWM_L_ON

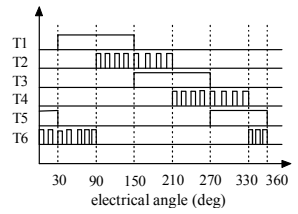

Fig.5. The logic trigger signal of each device in H_ON_L_ PWM

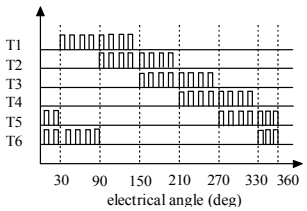

Fig.6. The logic trigger signal of each device in H_PWM_L_PWM

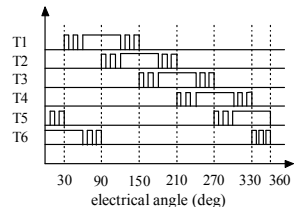

Fig.7. The logic trigger signal of each device in PWM_ON_PWM

Because H_PWM_L_PWM has more switching loss, the demand to the inverter heat dissipation performance is very high. The switching loss of each device is different in H_PWM_L_ON and H_ON_L_PWM and temperature is not uniform in the heatsink surface. According to the inverter heat dissipation performance, PWM_ON, ON_PWM and PWM_ON_PWM have higher reliability than H_PWM_L_ON,

H_PWM_L_PWM and H_ON_L_PWM.

B. Comparison of torque ripple in the six PWM methods

The commutation toque pulsation and switching frequency toque pulsation in PMBDCSCS is different in the each PWM method. H_PWM_L_PWM is the bipolar control and has larger switching frequency current pulsation than the other five PWM methods, so its switching frequency torque pulsation is the largest in the six PWM methods. H_PWM_L_ON has the same device logic trigger signal with PWM_ON from zero to 60^0 and with ON_PWM from 60^0 to 120^0 in the 120^0 conduction mode. H_ON_L_PWM has the same device logic trigger signal with ON_PWM from zero to 60^0 and with the PWM_ON from 60^0 to 120^0 in the 120^0 conduction mode. Therefore the torque pulsation in H_PWM_L_ON and H_ON_L_PWM is larger than in PWM_ON and ON_PWM. So PWM_ON, ON_PWM and PWM_ON_PWM are mainly studied and compared in the next.

Assuming that phase a will be turned off, phase b will be conducted, phase c is being in conduction, the inductance and CEMF are ideal, D is duty cycle. U_N is neutral point voltage. In the commutation process PWM_ON is the same with PWM_ON_PWM in the inverter output voltage equation. When the chopping device is off, the inverter output voltage equation in PWM_ON and PWM_ON_PWM can be expressed by:

$$U_A = 0 = E_A + L_A \frac{di_A}{dt} + R_A i_A + U_N \tag{1}$$

$$U_B = U_d \bullet D = E_B + L_B \frac{di_B}{dt} + R_B i_B + U_N \tag{2}$$

$$U_C = 0 = E_C + L_C \frac{di_C}{dt} + R_C i_C + U_N \tag{3}$$

The U_N in PWM_ON and PWM_ON_PWM is obtained as：

$$U_N = \frac{1}{2} U_d \bullet D \tag{4}$$

When the chopping device is off, the inverter output voltage equation in ON_PWM can be expressed by:

$$U_A = 0 = E_A + L_A \frac{di_A}{dt} + R_A i_A + U_N \tag{5}$$

$$U_B = U_d = E_B + L_B \frac{di_B}{dt} + R_B i_B + U_N \tag{6}$$

$$U_C = U_d \bullet (1 - D) = E_C + L_C \frac{di_C}{dt} + R_C i_C + U_N \tag{7}$$

The U_N in ON_PWM is obtained as：

$$U_N = U_d - \frac{1}{2} U_d \bullet D \tag{8}$$

When the chopping device is on, the inverter voltage output equation is the same in the PWM_ON, PWM_ON_PWM and ON_PWM. But the U_N is different in PWM_ON, PWM_ON_PWM and ON_PWM. According to (4) and (8), U_N in PWM_ON and PWM_ON_PWM is lower than in ON_PWM. According to (1) and (5), the current in phase a falls faster, the torque in phase a falls faster, but the rising velocity of phase b current is the same in PWM_ON, PWM_ON_PWM and ON_PWM, so the commutation torque pulsation is larger in ON_PWM.

In the non-commutation process, the two phases in the three-phase permanent magnet motor in 120^0 conduction mode is conducted and the other phase is shut off. Only one of two devices conducted is chopping. Now assuming that phase a is shut off, the current in phase b flows from inverter to the neutral point, the current in phase c flows from the neutral point to inverter, the each device is ideal, CEMF from the neutral point to inverter is defined as positive.

When phase a CEMF is more than zero and the chopping device S_2 is in off-state, the phase a voltage equation is

$$U_{S3} + U_{S1} = E_A - E_B - L_B \frac{di_B}{dt} - R_B i_B \tag{9}$$

When phase a CEMF is more than zero and the chopping device S_3 is in off-state, the phase a voltage equation is

$$U_d + U_{S2} + U_{S1} = E_A + E_C + L_C \frac{di_C}{dt} + R_C i_C \tag{10}$$

When phase a CEMF is less than zero and the chopping device S_2 is in off-state, the phase a voltage equation is

$$U_d + U_{S3} + U_{S4} = E_A + E_B + L_B \frac{di_B}{dt} + R_B i_B \tag{11}$$

When phase a CEMF is less than zero and the chopping device S_3 is in off-state, the phase a voltage equation is

$$U_{S4} + U_{S2} = E_A - E_C - L_C \frac{di_C}{dt} - R_C i_C \tag{12}$$

When phase a CEMF is more than zero and the chopping device is in on-state, the phase a voltage equation is

$$U_d - \frac{1}{2} U_d - U_{S1} = E_A \tag{13}$$

When phase a CEMF is less than zero and the chopping device is in on-state, the phase a voltage equation is

$$\frac{1}{2} U_d - 0 - U_{S4} = E_A \tag{14}$$

When the chopping device S_3 is in off-state, the voltage equation in the phase b and phase c is

$$U_{S2} + U_{S6} = E_B + E_C + L_B \frac{di_B}{dt} + L_C \frac{di_C}{dt} + R_B i_B + R_C i_C \tag{15}$$

When the chopping device S_2 is in off-state, the voltage equation in the phase b and phase c is

$$U_{S3} + U_{S5} = E_B + E_C + L_B \frac{di_B}{dt} + L_C \frac{di_C}{dt} + R_B i_B + R_C i_C \tag{16}$$

When the chopping device is in on-state, the voltage equation in the phase b and phase c is

$$U_d - U_{S3} - U_{S2} = E_B + E_C + L_B \frac{di_B}{dt} + L_C \frac{di_C}{dt} + R_B i_B + R_C i_C \tag{17}$$

According to (13) and (14) phase a has not freewheeling current when the chopping device is in on-state. If time trends to zero, (15) and (16) show that $L_B i_B / dt$ almost equals to $-E_B$ and $L_C i_C / dt$ almost equals to $-E_C$. When the chopping device is in off-state, the (9) and (12) show that phase a CEMF produces freewheeling current in phase a. The current is switching frequency pulsation current and causes the switching frequency torque pulsation. When the chopping device is in off-state, the (10) and (11) show that phase a CEMF does not produces freewheeling current in phase a and does not also produces the switching frequency pulsation torque. In the

non-commutation process, in order to eliminate the freewheeling current caused by phase a CEMF the chopping device in the PWM must be changed from S_2 to S_3 when the polarity of phase a CEMF change from positive to negative. PWM_ON_PWM has the change, therefore the torque pulsation caused by the phase a is eliminated. In principle the other non-commutation process is the same as the discussed process above.

So the torque performance in PWM_ON_PWM is the best, and the commutation frequency torque performance in PWM_ON is better than in ON_PWM.

C. Comparison of EMC and vibration in the three PWM methods

The PWM inverter based on switching operation has been considered as a representative noise source of conducted and radiated electromagnetic interference emissions. The conducted emission may interfere with other electronic equipment through power lines, while the radiated emission may bring malfunction, particularly to radio-controlled devices in the vicinity of the noise source. The system EMC is directly pertinent to the current pulsation in the inverter input filter inductor. The smaller the current pulsation is, the better the system EMC is. The current pulsation is the largest in H_PWM_L_PWM, and the system EMC in H_PWM_L_PWM is the worst. The system EMC in ON_PWM is better than in H_PWM_L_ON and H_ON_L_PWM. The EMC in PWM_ON and PWM_ON_PWM is better than in ON_PWM. The pulsation torque is the main source of the permanent magnet motor vibration. Thus according to the pulsation torque the sequence of the vibration performance is PWM_ON_PWM, PWM_ON, ON_PWM, H_PWM_L_ON (H_ON_L_PWM) and H_PWM_L_PWM from superiority to inferiority.

III. SIMULATION VERIFICATION

The PMBDCSCS is modeled in SABER and the permanent magnet motor is modeled in the circuit. The resistor, inductance and VCVS substitute stator resistor, winding inductance and phase CEMF. The permanent magnet motor parameters is: $P_n = 4.5kW$, $n_e = 400\ rpm$, $p = 4$, $E_A = 70\ V$, $L_A = 254uH$, $M_{AB} = 80uH$, $R_A = 0.03\Omega$. The switching frequency is 10kHz.The load is the propeller. In each figure the upper waveform is the simulation result in PWM_ON_PWM, the middle waveform is the simulation result in ON_PWM, the lower waveform is the simulation result in PWM_ON.

Fig.8 and Fig.9 prove that the torque performance in PWM_ON_PWM is the best and the commutation ripple torque in PWM_ON is better than in ON_PWM. Fig.11 indicates that the commutation frequency harmonic current magnitude in the inverter dc input filter inductor in PWM_ON_PWM and PWM_ON is smaller than in ON_PWM. Fig.10 indicates that the switching frequency harmonic current magnitude in the inverter dc input filter inductor in PWM_ON_PWM , PWM_ON and ON_PWM is almost the same. Fig. 12 proves that there is not switching frequency pulsating current caused by phase CEMF in the inactive phase in PWM_ON_PWM.

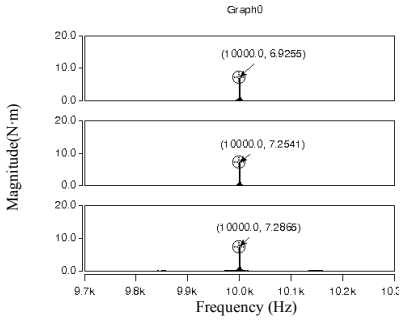

Fig.8.harmonic torque spectrum in the vicinity of switching frequency

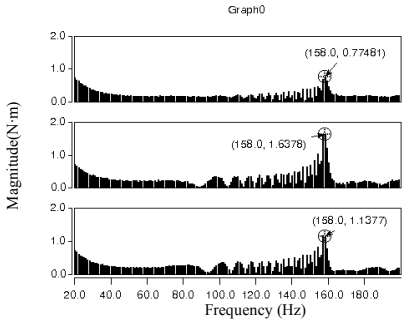

Fig.9. harmonic torque spectrum in the vicinity of commutation frequency

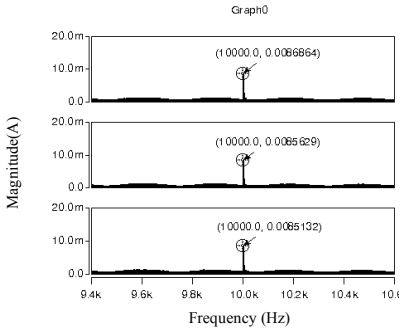

Fig.10. harmonic current spectrum of the inverter dc input filter inductor in the vicinity of switching frequency

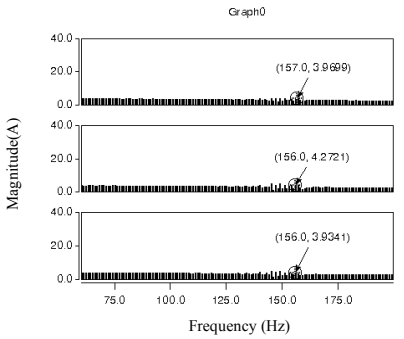

Fig.11. harmonic current spectrum of the inverter dc input filter inductor in the vicinity of commutation frequency

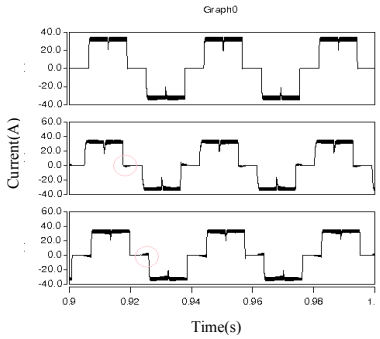

Fig.12. phase a current

IV. CONCLUSION

Through the theoretical analysis and simulation verification the six PWM methods are compared in the efficiency, reliability, torque ripple, EMC and vibration. The comprehensive performance sequence from superiority to inferiority is PWM_ON_PWM, PWM_ON, ON_PWM, H_PWM_L_ON (H_ON_L_PWM) and H_PWM_L_PWM from the system point of view. The conclusion conduces to the system design in the engineering practice and especially to the multiphase motor drive system.

REFERENCES

[1] Joong H S, Ick C, Commutation Torque Ripple Reduction in Brushless DC Motor Drives using a single DC current sensor[J]. IEEE transactions on power electronic, 2004 19(2), pp.312-219

[2] Renyuan Tang, Modern Permanent Magnet Machines—Theory and Design, CHINA MACHINE PRESS, December 1997.

[3] Bimal K. bose, Modern Power Electronics and AC Drives, CHINA MACHINE PRESS, January 2003.

[4] Yoshihiro murai, Yoshihiro kawase, etc, Torque Ripple Improvement for Brushless DC Motor Miniature Motors, IEEE transactions on industry application, Vol.25, No.3 May/June 1989，pp.441- 450

[5] Xinghua Wang, Qingfu Li, Shuhong Wang, Analysis of the Commutation Torque Ripple of Permanent Magnet Brushless DC Motors, JOURNAL OF XI'AN JIAO TONG UNIVERSITY , Vol.37, No.6 June 2003, pp.612-616